

Development of a Composite Boom Robotic Arm for Space Applications

Preston Wang

Abstract—A novel robot design called Reachbot involves using several extendable bistable composite slit tubes (called booms) for locomotion and manipulation. Booms are lightweight composite tubes that can be unfurled to long lengths on the order of several meters from a rolled up configuration. They are lightweight, compact yet strong, making them ideal for space applications. Previous applications have used them as space structures but this paper presents a novel application of composite booms as arms of a space robot. A simple mechanical design was created for initial testing of the boom. The design demonstrated extension, retraction and rotation of the boom with a gecko-adhesive gripper. In addition, a rigid and flexible model of the boom were generated for control and trajectory optimization. The flexible model was compared to a simple rigid model for two use cases: moving an object between points and capturing a spinning object. Results indicated that a rigid model is suitable for large time scale planning but a flexible model is needed to capture impact and shock loading dynamics involved in grasping a spinning object.

I. INTRODUCTION

Space robotics is an emerging field and presents many opportunities for innovation and development. New robots are needed for space exploration, satellite servicing, space station maintenance, multirobot coordination, and numerous applications.

A novel robot design called Reachbot involves using several extendable bistable composite slit tubes (called booms) for locomotion and interaction with the environment (Fig. 1). Booms are lightweight composite tubes that can be unfurled to long lengths on the order of several meters from a rolled up configuration. They are lightweight, compact yet strong, making them ideal for space applications. Booms have already been used in several space structures applications such as deployable masts, space imaging [1], solar sails [2] and de-orbiting [3]. In these applications, the boom is deployed once from a reeled up configuration. This paper presents a new application of these booms as arms of a space robot, where the boom's length and orientation are controlled. Using booms as robotic arms presents several advantages. Their strength in tension grants a robot increased wrench and manipulation capability. At the same time, they can be deployed to long lengths, which would enable a small robot platform to have a large reach. By using the booms for both manipulation and locomotion, a small robot platform (Reachbot) can now achieve high manipulation and high mobility. However, these benefits come with several caveats. At the boom's long deployment length, the booms become more flexible. Control laws and trajectory plannings will need to account for the boom's flexibility in order to generate optimal trajectories and robust control. In addition,

the boom's slenderness means that the robot will be operating at the boom's structural limits and careful consideration planning is needed in order to keep the booms within these limits.

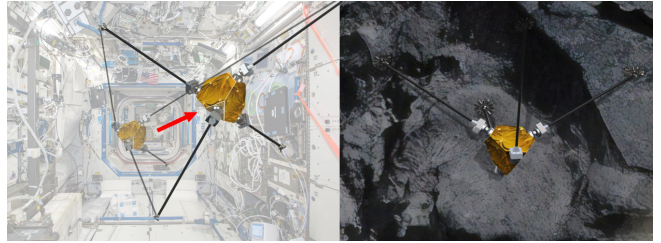


Fig. 1: Left: Reachbot shown on the ISS performing maintenance tasks. Right: Reachbot shown traversing a lunar lava tube

A. Literature Review

Several robots have been developed for space applications and generally fall under two categories: large dexterous robots and small free-flyers/rovers, with smaller free-flyers being more recently developed (Fig. 2). Previous examples of large dexterous robots include the Canadarm and Dextre [4], which are used for servicing on board the International Space Station (ISS). Robonaut was developed by NASA as a humanoid robot to advance anthropomorphic robotic systems and dexterous manipulation [5]. An upgraded version of Robonaut (Robonaut 2) was later developed with improved range of motion and dexterity [6]. Despite their impressive manipulation capability, these robots are bulky, complex, and have limited mobility. On the other side of the spectrum are small free-flyer platforms. Small free-flyers are a recent development and used for intravehicle operations on the ISS. Notable examples include SPHERES [7], Int-Ball by JAXA [8] and Astrobee [9], [10]. These free-flyers have been used as research platforms and for crew surveillance. While mobile and lightweight, they have limited manipulation capability.

For planetary exploration of extreme terrain, there is a similar spectrum from robots with greater manipulation capability to robots with high mobility. LEMUR3 sits on the manipulation side of the spectrum with multiple joints that enable it to vertically traverse rocky terrain [11]. Axel sits on the other side of the spectrum with high mobility to descend down rocky terrain but with very limited manipulation capability [12].

On the control side, control of flexible structures has been a topic of research for many years. This topic was especially prevalent in the mid 80s to 90s for the control of large

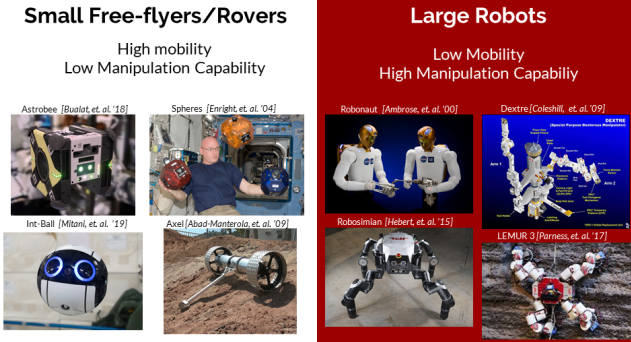


Fig. 2: Comparison of different robot architectures

space truss structures. A survey of these work highlighted the challenges in modeling a large flexible system, identifying optimal sensor location and ensuring closed-loop stability in the midst of model uncertainty. One of the more promising approaches involved incorporating a FEM model of the structure, performing model reduction to reduce the state space and decomposing the model into substructures for control [13]. Another approach is the Assumed Modes Method (AMM) where the basis functions for the mode shapes of the structure are defined a priori [14]. The accuracy of the approach can be improved by using quadratic mode shapes. A simple FEM approach with a few elements and AMM approach were compared for control on two different beams with different stiffnesses [15]. Both approaches provided a valid model of the flexible beams and could be used to control the beam.

B. Motivation of proposed work

The Reachbot platforms provides a novel intersection of mobility and manipulation through using extendable booms for mobility and manipulation. It is a new application of recent advances in lightweight space structures. Bi-stable composite booms have been used in structural applications but have not been implemented in this dynamic function as a robotic arm. Using composite booms in this new application first requires designing mechanisms that can control the length and orientation of the boom. Previous applications of composite booms only had to ensure that the boom fully deployed and did not have to modulate the length of the boom. In addition, new controllers are needed to account for the boom's flexible dynamics and structural limits.

C. Statement of work

In this paper, we introduce the design of a new composite boom robotic arm for space application. An initial prototype of the arm was developed that demonstrated the ability to extend, retract, maintain a constant length, and reorient the boom. Additionally, rigid and flexible models of the boom was developed and implemented in trajectory optimization for several potential use cases: moving an object between points, and grasping a tumbling object.

II. PROBLEM FORMULATION

Designing a new composite boom arm presents a twofold problem: a mechanical design capable of actuating the boom and a trajectory generator capable of generating optimal

trajectories. On the mechanical design side, the design must accomplish the following objectives:

Mechanical Design Objectives

- 1) Extend and retract the boom
- 2) Reorient the boom's angle
- 3) Maintain the boom's angle and position
- 4) Interface with a gripper at the end of the boom

On the trajectory side, the algorithm must accomplish the following objectives:

Trajectory Objectives

- 1) Capture the boom's flexible dynamics in an appropriate model.
- 2) Generate a trajectory subject to the boom's dynamics and within the motor torque limits
- 3) Generate trajectories for several use cases
 - a) Moving an object between points
 - b) Grasping a tumbling object

III. PROPOSED SOLUTION

An initial prototype of the arm was developed with Rolatube mast systems which were readily available online (Fig. 3). These booms are used in defense applications as makeshift ladders and masts for radio antennas. They have the same bi-stable characteristic as space grade bi-stable composite booms. However, they have a more robust design and consequently are more rigid. Nevertheless, they still provide a means to develop an initial prototype and develop initial algorithms for trajectory optimization. Specifically, the 2" diameter and 2m length booms were used for this initial prototype.

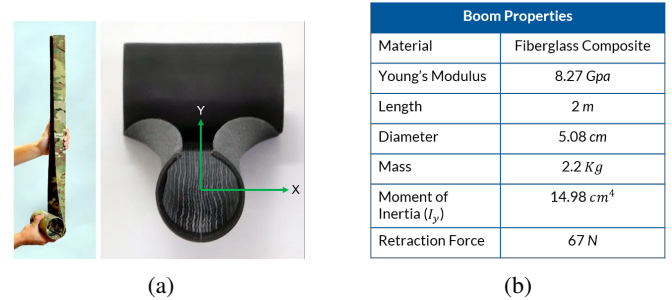


Fig. 3: (a) Rolatube boom showed being deployed from reeled configuration to unrolled slit-tube configuration. (b) boom material, and mechanical properties used in the design

A. Mechanical Design

With the initial prototype, the primary design philosophy was to have the simplest design in order to have a working prototype as quickly as possible. The resulting design was completed in 7 weeks from initial concept to working prototype (Fig. 4), with two design iterations. For simplicity, most components were purchased through McMaster or laser cut out of Duron sheets. The assembly is then attached to 8020 rails as a sturdy base. The resulting arm is a planar arm with two degrees of freedom: extension/retraction and

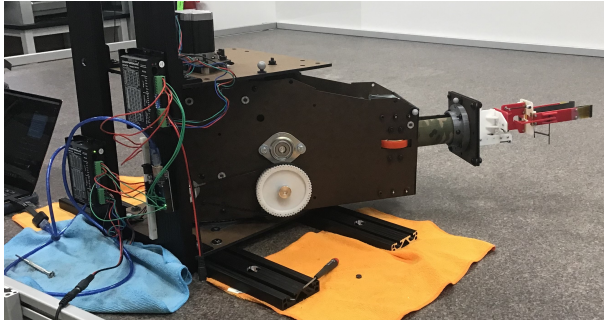


Fig. 4: Initial Prototype shown on a granite table at Stanford's Space Robotics Facility

rotation (Fig.5). A previously designed passive gripper by Estrada et. al is attached to the end of the arm [16]. This gripper features gecko-inspired dry adhesives and a bi-stable mechanism that triggers upon contact to grasp an object.

1) Actuation

Two NEMA 23 stepper motor with a max torque of 1.9 Nm were used to actuate the boom's extension and rotation. Stepper motors were chosen for their low cost, high torque, and simplicity for control. The required torque was determined through measuring the force needed to roll-up the boom. The measured retraction force was 67 N.

For actuation in translation, a motor drove a rubber roller via a belt and pulley drive system (Fig. 5 6). A belt and pulley drive system was chosen in order to place the motor closer to the axis of rotation to minimize the inertia of the system. The active rubber roller is opposed by a passive rubber roller to increase the roller's grip on the boom. Several other rollers and wheels are also used to constrain the boom. Three wheels at the output provide lateral and vertical constraint. Rollers around the spool help the boom roll up during retraction. For rotation, a simple spur gear drive system was used. The carriage sits on two turntables which are used facilitate rotation and support the cantilevered arm.

2) Electronics

The two motors are each controlled by a stepper motor driver, which allow for micro-stepping for fine position control. An Arduino micro-controllers receives velocity command from the computer and sends Pulse Width Modulation (PWM) signals to the driver to adjust the stepper motor velocity.

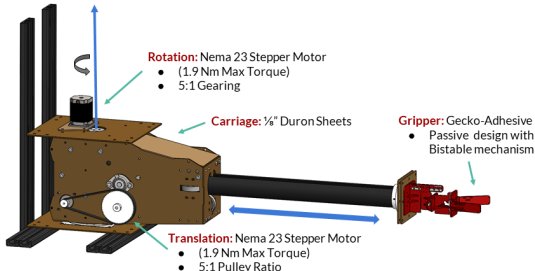


Fig. 5: Mechanical Design of arm, specifying means of actuation

B. Modeling

A rigid model and flexible model were developed for the system (Fig. 7). The rigid model serves as a base model and a point of comparison. Due to their lengths, the booms flexibility becomes an important aspect to consider in the modeling of this robotic arm. Both models assume that the gripper's dynamics can be ignored and that friction is negligible. While the gripper dynamics play an important role in grasping an object [16], these initial models ignored the gripper dynamics. The main purpose of these models is to capture the dynamics of the boom to gain an understanding of the boom's behavior. The gripper and the object being grasped are combined into a single point mass with a constant orientation and offset from the end of the boom. The carriage is modeled as a mass with rotational inertia (J_c). The boom is modeled as a continuous beam with linear density (ρ) and the reel is considered to coincide with the rotation axis. As the boom's length increases, the center of mass shifts along the boom's axis away from the center of rotation via the following equation for $\gamma(t)$. Correspondingly, the end mass location along the boom's axis is given by $\lambda(t)$.

$$\gamma(t) = \frac{\rho(L(t) + a)}{M_{boom}}, \lambda(t) = L(t) + a + B \quad (1)$$

1) Rigid Model

The arm is modeled in a 2D plane as an arm with a rotary joint and prismatic joint. It is characterized by 4 states: $x = [L(t), \theta(t), \dot{L}(t), \dot{\theta}(t)]$ and two inputs $u = [F_L, F_\tau]$ where F_L and F_τ are the torque for extension/retraction and rotation respectively. With these states and inputs, the equations of motions can be derived. An Euler-Lagrange formulation was chosen to derive the equation of motion. The model was broken up into three inertial elements: the end mass, the boom, and the carriage. The position of the end mass and the boom are defined as follows:

$$x_{end} = \lambda(t)\cos(\theta(t)), y_{end} = \lambda(t)\sin(\theta(t)) \quad (2)$$

$$x_{boom} = \gamma(t)\cos(\theta(t)), y_{boom} = \gamma(t)\sin(\theta(t)) \quad (3)$$

The Lagrangian is then defined as:

$$L = \frac{1}{2}M_{end}(\dot{x}_{end}^2 + \dot{y}_{end}^2) + \frac{1}{2}M_{boom}(\dot{x}_{boom}^2 + \dot{y}_{boom}^2) + \frac{1}{2}J_c(\dot{\theta}^2(t)) \quad (4)$$

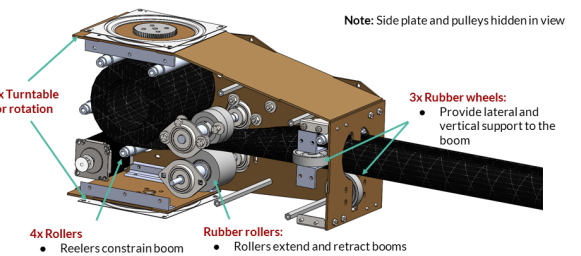


Fig. 6: Section view of arm showing the internal mechanism for extending and retracting the boom

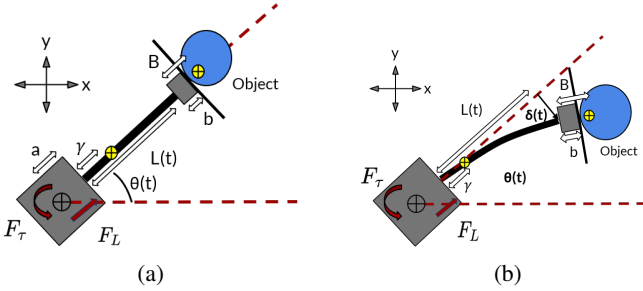


Fig. 7: (a) Rigid model of the boom (b) Flexible Model of the Boom.

Using Euler-Lagrange equations, results in the following equation of motions.

$$\ddot{L}(t)(M_{end} + \frac{\rho^2}{M_{boom}}) - \gamma(t)\dot{\theta}(t)^2 + \lambda(t)M_{end} = F_L G_L \quad (5)$$

$$\ddot{\theta}\left(\frac{a^2\rho^2 + 2a\rho^2L(t)}{M_{boom}} + M_{end}(A + L(t))^2 + J_c + \frac{\rho^2L(t)^2}{M_{boom}}\right) + 2L(t)^2\dot{\theta}\left(\frac{\rho^2(a + L(t))}{M_{boom}} + M_{end}(A + L(t))\right) = F_\tau G_\tau \quad (6)$$

2) Flexible Model

To capture the boom's flexibility, Euler-Bernoulli beam theory is employed. Previous literature have employed more advanced model such as FEM, ROM [17], and AMM with quadratic displacements [15]. However, because of the Rolatube boom's high stiffness, a simple beam model is used instead. This model also corresponds to an AMM method with linear displacements. The boom is modeled as a cantilever beam with a tip mass at an offset (B) from the end of the boom. The tip mass included both the mass of the object and the gripper. Inertial forces on the tip mass during rotation creates a force and a moment on the end of the boom which results in a corresponding deflection (δ). The additional moment comes from the offset of the mass from the end of the boom. Using the principle of superposition, the deflection contribution from the force and moment respectively (Eq. 7) can be summed together to find the total deflection (Eq. 8). The boom deflection can be modeled as a linear spring with the deflection stiffness (K) derived from the force to deflection ratio.

$$\delta_F = \frac{FL(t)^3}{3EI}, \delta_M = \frac{FBL(t)^2}{2EI} \quad (7)$$

$$\delta = \delta_F + \delta_M \quad (8)$$

$$K = \frac{6EI}{L(t)^2} \left(\frac{1}{2L(t) + 3B} \right) \quad (9)$$

Because of the deflection, the location of the end position needs to be modified to the following equation.

$$x'_{end} = \lambda(t)\cos(\theta(t)) - \delta(t)\sin(\theta(t)) \quad (10)$$

$$y'_{end} = \lambda(t)\sin(\theta(t)) + \delta(t)\cos(\theta(t)) \quad (11)$$

In addition to the new end position, the Lagrangian also needs to be updated with the potential energy from the flexible beam, resulting in the following Lagrangian.

$$L = \frac{1}{2}M_{end}(\dot{x}_{end}^2 + \dot{y}_{end}^2) + \frac{1}{2}M_{boom}(\dot{x}_{boom}^2 + \dot{y}_{boom}^2) + \frac{1}{2}J_c(\dot{\theta}^2(t) - \frac{1}{2}K(\delta(t))^2) \quad (12)$$

The states vector is augmented with 2 more states, resulting in a 6 state system: $x = [L(t), \theta(t), \delta(t), \dot{L}(t), \dot{\theta}(t), \dot{\delta}(t)]$. From this new Lagrangian, a third second order equation is produced that accounts for the boom's deflection.

$$M_{end}\ddot{\delta}(t) + C\dot{\delta}(t) + K\delta(t) = M_{end}(2L(t)\dot{\theta}(t) + \lambda(t)\ddot{\theta}(t)) \quad (13)$$

This is equivalent to a 2nd order differential equation for a simple harmonic oscillator with the external force from the inertial forces on the end mass. Rayleigh damping is used to define the damping coefficient as follows [18], [19]:

$$C = \alpha M_{end} + \beta K \quad (14)$$

$$\alpha = 2\xi\omega, \beta = 0, \omega = \sqrt{\frac{3EI}{M_{end}L(t)^3}} \quad (15)$$

ω is the first natural frequency of the boom at that particular length and ξ is a damping coefficient parameter that can be adjusted.

3) Grasping Spinning Object Model

Lastly, a model of grasping a spinning object was developed. The model and the object parameters used were based off the work by Estrada et. al [16]. They had run several tests of grasping a spinning object with their passive gripper. The grasp is modeled as an inelastic collision where the object perfectly "sticks" to the gecko-adhesive gripper. With this model, all of the rotational momentum of the object is transferred to the combined system. The object starts with some initial angular velocity (Ω_o) and the arm contacts the object with 0 angular velocity. Through conservation of angular momentum, the resulting angular velocity of the system becomes as follows.

$$\Omega_f = \frac{I_o\Omega_o}{I_f} \quad (16)$$

$$I_f = I_o + m_o(\lambda(t) + r_o)^2 + J_c + m_{gripper}\lambda^2(t)) \quad (17)$$

This calculated angular velocity applies to both the rigid and the flexible model. However, in the case of the flexible model, an initial δ deflection is also added imparted into the boom due to the force from grasping the spinning object. The deflection can be calculated from the dissipation of kinetic energy during the collision. Although gripper dynamics are ignored, the gripper itself also has springs and dampers which would absorb a significant portion of the dissipated kinetic energy. To account for the gripper's stiffness and damping, a ratio (η) was added.

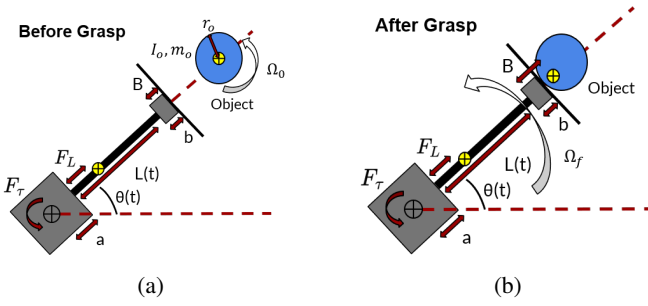


Fig. 8: Model of grasping a spinning object, initially spinning with rotational velocity Ω_0 . The diagram shows a rigid boom but the principle applies to both the rigid and flexible model.
(a) Before grasping occurs (b) After grasping the object

Control

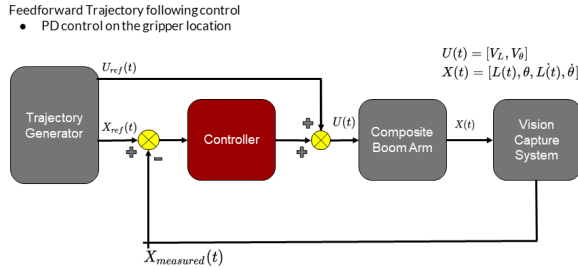


Fig. 9: Block Diagram of Feed Forward Trajectory Following Control System

$$\delta_{grasp} = \sqrt{\frac{(I_o\Omega_o^2 - I_f\Omega_f^2)\eta}{K}} \quad (18)$$

C. Control

In order to control the system, a feed forward trajectory following control system design was selected (Fig. 9). The trajectory optimization algorithm generated a reference trajectory of the states and a reference control. The reference control were the velocities for the two motors, which are running under a speed controller. Measured data from the vision capture system provided a feedback loop to the controller. The controller itself was a simple PD controller for the motor speeds.

D. Trajectory Optimization

Trajectory optimization was performed through an iterative Linear Quadratic Regular (iLQR) algorithm. iLQR was chosen for it's simplicity of implementation and it's ability to handle non-linear dynamics through local linearization of the non-linear dynamics. A quadratic cost function was defined for the algorithm with cost taken relative to the goal state (x_{goal}).

$$J = \frac{1}{2}(x - x_{goal})^\top Q(x - x_{goal}) + \frac{1}{2}u^\top Ru \quad (19)$$

The motors also have torque limits that must be maintained. In order to keep the torques within the specified limits, a squashing function was implemented on the torque (Fig. 10). The control limits were scaled down from the motor torque limits by an appropriate safety factor.

$$u_{constrain} = \tau_{max} * \text{Tanh}(u), \tau_{max} = \frac{\text{Max Torque}}{\text{Safety Factor}} \quad (20)$$

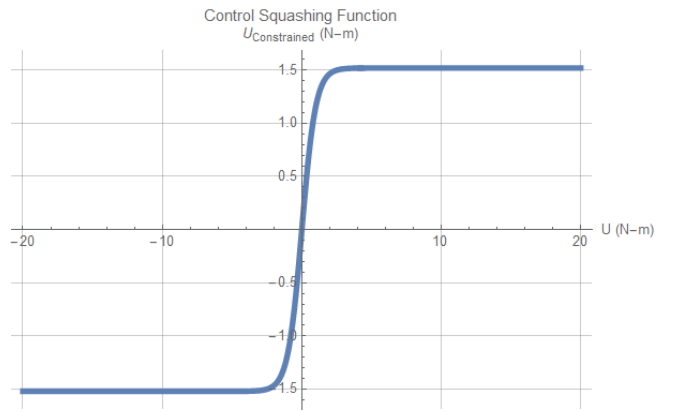


Fig. 10: Squashing function on the Motor Torque

An iLQR package developed by Anass based off Tassa et al [20], was used for solving the iLQR problem.

IV. SIMULATION/EXPERIMENTS

A. Mechanical Hardware

The robot arm was successfully assembled together and demoed under extension/retraction, and rotation. In addition, the arm successfully grasped an object (a water bottle), and moved it from point to point (Fig. 11). During this movement, the arm displayed significant deflection under torsion. The boom's cross-section makes it significantly susceptible to torsional modes as compared to bending and axial modes. Torsional modes become especially apparent when the object's center of mass is not aligned to the boom's center axis. Future arm designs will need to take factor in the torsional weakness.

B. Trajectory Optimization

Trajectory Optimization was performed for two cases: moving an object from point to point and grasping a spinning object. For both cases, both the rigid model and flexible model were used and the results were compared to each other. In addition the same cost matrices (Q and R) were used for both models to facilitate comparison. The spinning object parameters were taken from [16]. Under the moving an object from point to point case, the cost matrices were weighed more heavily on the position terms ($L(t), \theta(t)$). Under the grasping a spinning object case, the cost matrices were weighed more heavily on the velocity terms ($\dot{L}(t), \dot{\theta}(t)$). The main objective of this case is to stabilize the system, bringing the system to rest. Control sequences for both cases were generated via a random number generator.



Fig. 11: Robot Arm grasping a water bottle

1) Moving Object between points

Simulations were conducted for moving an object from an initial position at angle 0 deg with respect to the x-axis to a goal position at 90 deg. The starting and ending lengths were the same and simulations were ran at "short" (0.5 m), "medium" (1 m) and "long" (1.5m) arm lengths (Fig. 12). Surprisingly, there was little deviation between the rigid and flexible models (Fig. 13). On the trajectory side, there was only differences in position on the order of less than 1 mm. On the control side, the rotational torque profile was nearly the same between rigid and flexible models (Fig. 14). However, there were some deviations in the translational torque, especially some initial oscillations in motor torque for the flexible model. This can be attributed to the algorithm attempting to stabilize the boom's deflection from the initial torque input.

At first, the small deviations were attributed to the boom's rigidness. As shown, the boom's have minimal deflection, even at the longest length, with a maximum deflection around .4mm (Fig. 15). However, follow-up experiments at a smaller moment of inertia, corresponding to a smaller diameter boom, revealed similar results. The moment of inertia was reduced to 10% of the original value and the exact same simulations were ran. The subsequent results revealed similar trajectories (Fig. 16) and torque profiles despite having greater tip deflection (Fig. 17). Nevertheless, deflections were still around the same order of magnitude as before (Fig. 18).

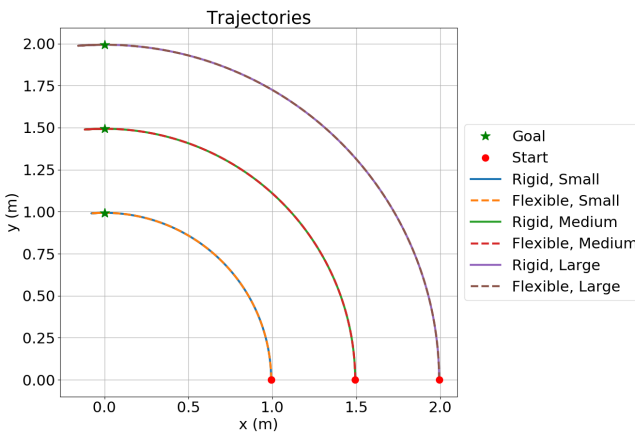


Fig. 12: Comparison of boom trajectories for rigid and flexible models. Booms are initialized at various locations along the x-axis and given a goal location along the y-axis

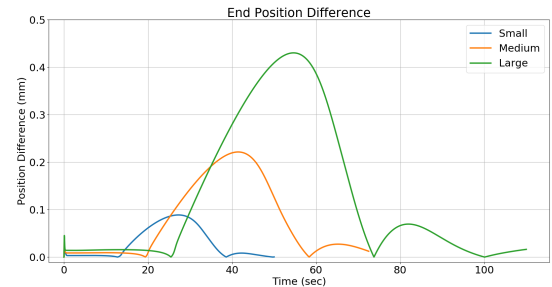


Fig. 13: Difference between flexible and rigid model end positions for various lengths of the boom.

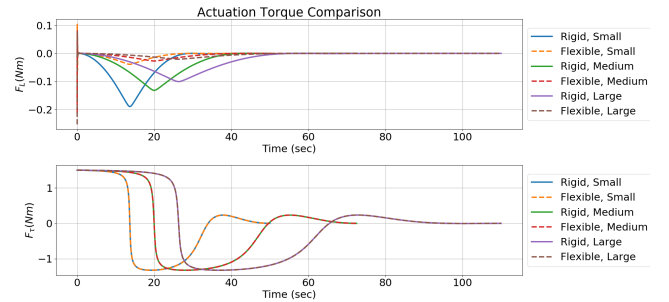


Fig. 14: Comparison of actuation torques for rigid and

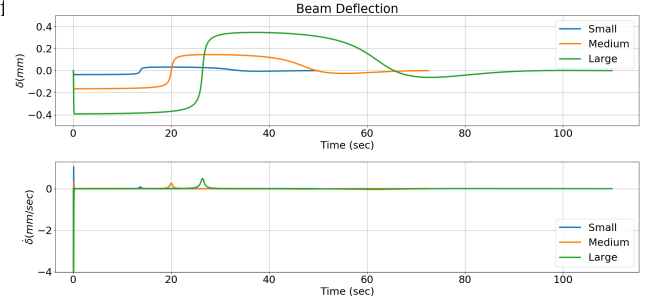


Fig. 15: Comparison of boom deflections at various lengths of the boom.

While initially surprising, these results actually align with intuition. A boom's flexibility, is not as noticeable as long as the arm experiences minimal tangential acceleration. Little acceleration translates to minimum inertial forces, which in result correspond to minimum tip deflections. Achieving small acceleration is possible by rotating at small angular rates and minimizing changes in angular velocity.

In addition, the length of the simulation had a significant impact on whether the algorithm would converge to a trajectory that could bring the object from start to goal (Fig. 19). During initial trials, the length of the trajectory had to be adjusted in order to help the algorithm converge. Tassa et. al also noted that the length of the horizon plays a vital role in the convergence of the algorithm [20]. One factor is the motor torque limit, which limits the maximum acceleration and deceleration of the boom. This will vary depending on the object mass and the length of the boom. Another factor is shortening the simulation would consequently require greater accelerations and velocities. However, since the costs penalize deflections, the algorithm would in turn minimize accelerations to keep the deflections small. If the cost on the

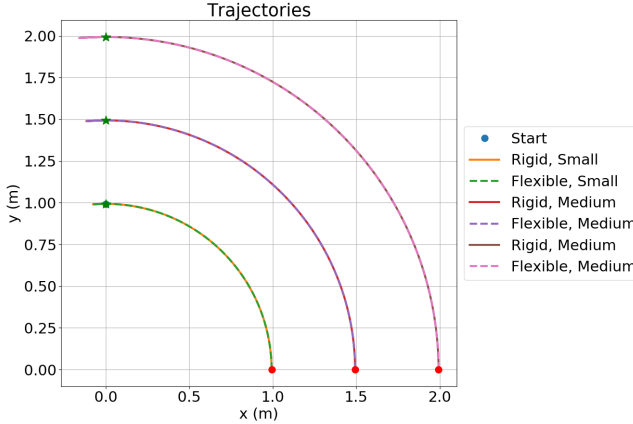


Fig. 16: Comparison of boom trajectories for rigid and flexible models with reduced moment of inertia

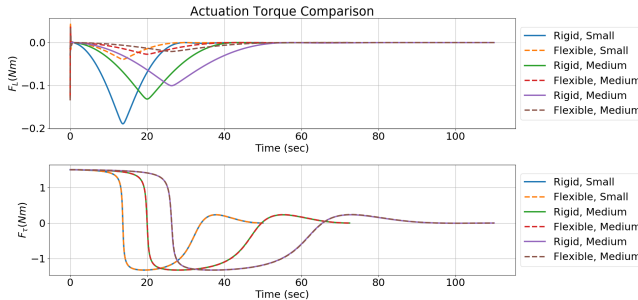


Fig. 17: Comparison of actuation torque for rigid and flexible models with reduced moment of inertia

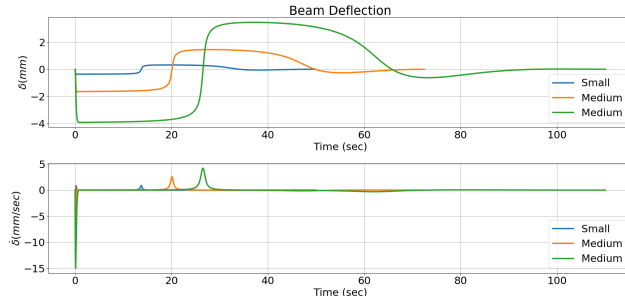


Fig. 18: Boom deflections with reduced moment of inertia deflection is reduced, then there is an increased possibility that the system will become unstable. Hence, tuning the time horizon becomes an important factor to ensure control stability and convergence.

2) Grasping Spinning Object

Simulations were conducted for grasping an object rotating at 1 rev/sec and 2 rev/sec. The arm contacts the object at a length of 1m with a small linear velocity. Post collision, the combined object-arm system has an initial velocity ($\dot{L}(t)$) and rotational velocity ($\dot{\theta}(t)$). The algorithm's objective is to stabilize the system which is defined as bringing the system to 0 linear and rotational velocity. Unlike the previous case, the boom's stiffness plays a more prominent role in the system's behavior when grasping a spinning object. Figure 20 present the corresponding trajectories for a boom with nominal stiffness and a boom with 10% of the nominal moment of inertia.

Although outward similar, the corresponding motor torque

Moment of Inertia = 14.98 cm ⁴	Small	Medium	Large
Time (sec)	50	72.5	110
Final Position Error (Rigid) (mm)	2.9	5.3	1.7
Final Position Error (Flexible) (mm)	2.9	5.3	1.7

Moment of Inertia = 1.498 cm ⁴	Small	Medium	Large
Time (sec)	50	72.5	110
Final Position Error (Rigid) (mm)	2.9	5.3	1.7
Final Position Error (Flexible) (mm)	2.9	5.3	1.7

Fig. 19: Time to convergence and position error from target goal

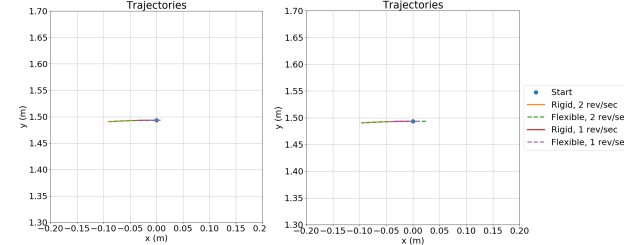


Fig. 20: Comparison of boom trajectories of grasping a spinning object for both rigid and flexible models. Left plot shows the trajectory for a boom with nominal moment of inertia. Right plot shows the trajectory of a boom with reduced moment of inertia

(Fig. 21 & 22) and deflections (Fig. 23 & 24) reveal a more noticeable disparity. The disparities can be attributed to the deflection of the boom from the contact forces. A less rigid boom, will have greater tip deflection. The boom with a reduced moment of inertia experienced 20mm of deflection whereas the nominal boom only experienced 8mm of deflection. These deflections play an important role in the resulting torque profile needed to stabilize the system. As such, the flexible dynamics must be included in the trajectory planning when contact dynamics are involved.

V. CONCLUSIONS

This paper demonstrated a new prismatic robot arm concept using bi-stable composite booms. Bi-stable booms provide a means for achieving a lightweight structure that can be used for mobility and manipulation in space. The development of this arm is a stepping stone for the further development of a new robot concept called Reachbot. Reachbot aims to bridge the gap between small free-flyer type robots and large dexterous robot by combining both mobility and

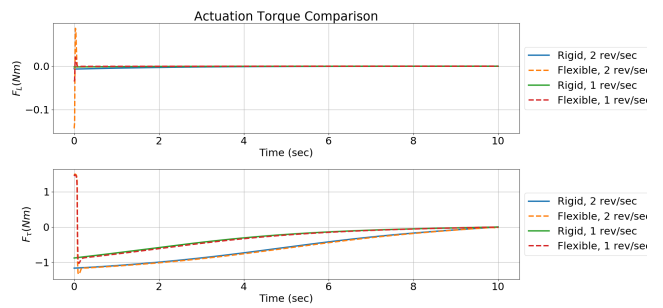


Fig. 21: Comparison of motor torques while stabilizing a spinning object

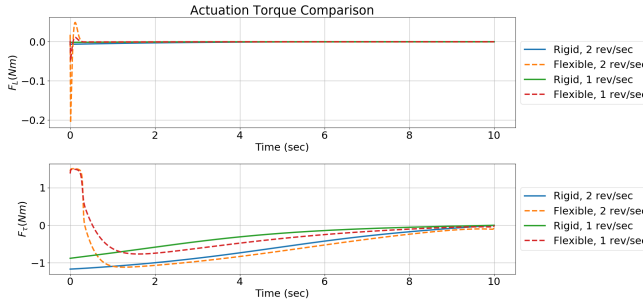


Fig. 22: Comparison of motor torques while stabilizing a spinning object with a reduced moment of inertia boom

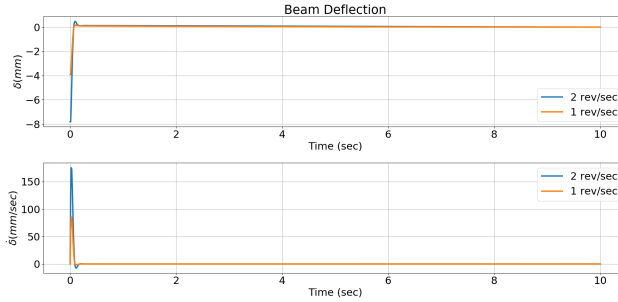


Fig. 23: Boom deflections after grasping a spinning object

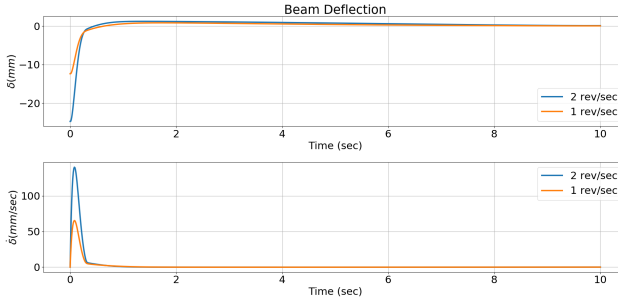


Fig. 24: Deflections of a reduced moment of inertia boom after grasping a spinning object

manipulation in a small robotic frame. An initial prototype was developed in order to gain insight into the concept of using booms in this novel application.

A. Mechanical Design:

From the initial prototype, several key lessons were learned. Firstly, the slit-tube shaped booms were found to be weak in torsion. One method to handle this weakness is to design a gripper that can adjust its orientation such that the object's center of mass is aligned to the boom's center axis. Such design can be pursued either through regrasping strategies or with a passive mechanism. Another solution is to pursue alternative boom cross-sections that have greater torsional stiffness. Lastly, trajectory algorithms could be

designed to account for the torsional weakness and minimize the torsional deflection of the arm.

B. Trajectory Optimization:

On the trajectory optimization side, rigid and flexible models had similar trajectories and control when moving an object between points. We hypothesized this behavior occurred because the controller ended up taking trajectories with minimal acceleration and velocities where the flexibility of the boom did not play a significant role. While, it may be possible to ignore the flexibility of the boom in this aspect, one must still take into account the flexibility of the boom in order to prevent instability. Further analysis is needed to determine the stability of the system if a purely rigid model is to be used.

When grasping a spinning object, the boom's flexibility did play a significant role. The stiffness of the boom directly affected how much deflection the boom experienced and how much energy is transferred into the boom versus into the gripper. For the purposes of this paper, the gripper dynamics were ignored. However, future analysis should incorporate the gripper dynamics to capture the full behavior when grasping a spinning object. This results applies to other potential contact or shock loading situations such as perching against a wall or pulling a velcroed item.

With these findings, a potential design for the motion planning and control system is to use a rigid model for planning motion between way points and a flexible model for contacts. The rigid model is simpler and will require less computational resources. Then, the planner and controller can switch over to the more complex and computationally taxing flexible model when needed. Criteria will need to be developed for when to optimally switch between rigid and flexible models.

C. Future Work

These initial insights also opened up a wealth of other research opportunities such as guaranteeing safety or predicting and adapting to unknown object parameters. Guaranteeing safety is a major concern for space applications. A robot working on the international space station would need to guarantee that it does not accidentally trigger a switch or collide with another object. In addition, the boom's long length makes it susceptible to bending and buckling loads. The controller would need to guarantee that the arm stays within its mechanical limits at all times. There are also numerous potential objects that an object might grab. These objects will most likely have unknown system parameters. As such, the controller must be able to predict and adapt to these unknown parameters. On the mechanical side, improvements can be made to the current passive gripper to allow for use

in other use cases such as perching against a wall, pulling an object, or interfacing with a control panel.

Lastly, this work has focused on a single arm. Reachbot will incorporate several arms and the integration of several arms into one platform will be another project in and of itself. Through all these developments, I hope that robot technology would be advanced to further extend a robot's reach in outer space.

REFERENCES

- [1] Joseph N Footdale and Thomas W Murphey. Mechanism Design and Testing of a Self-Deploying Structure Using Flexible Composite Tape Springs. In *Proceedings of the 42nd Aerospace Mechanisms Symposium*, pages 1–13, 2015.
- [2] Juan M Fernandez. Advanced Deployable Shell-Based Composite Booms For Small Satellite Structural Applications Including Solar Sails. In *International Symposium on Solar Sailing*, number March, page 19, 2017.
- [3] Craig Underwood, Andrew Viquerat, Mark Schenk, Simon Fellowes, Ben Taylor, Chiara Massimiani, Richard Duke, Brian Stewart, Chris Bridges, Davide Masutti, and Amandine Denis. The inflatesail CubeSat mission – The first European Demonstration of Drag-Sail De-Orbiting. In *Advances in the Astronautical Sciences*, volume 163, pages 261–278, 2018.
- [4] Elliott Coleshill, Layi Oshinowo, Richard Rembala, Bardia Bina, Daniel Rey, and Shelley Sindelar. Dextre: Improving maintenance operations on the International Space Station. *Acta Astronautica*, 64(9–10):869–874, 2009.
- [5] Robert O. Ambrose, Hal Aldridge, R. Scott Askew, Robert R. Burridge, William Bluethmann, Myron Diftler, Chris Lovchik, Darby Magruder, and Fredrik Rehnmark. Robonaut: NASA's space humanoid. *IEEE Intelligent Systems and Their Applications*, 15(4):57–62, 7 2000.
- [6] M. A. Diftler, J. S. Mehling, M. E. Abdallah, N. A. Radford, L. B. Bridgwater, A. M. Sanders, R. S. Askew, D. M. Linn, J. D. Yamokoski, F. A. Permenter, B. K. Hargrave, R. Platt, R. T. Savely, and R. O. Ambrose. Robonaut 2 - The first humanoid robot in space. In *Proceedings - IEEE International Conference on Robotics and Automation*, pages 2178–2183, 2011.
- [7] John Enright, Mark Hilstad, Alvar Saenz-Otero, and David Miller. The SPHERES guest scientist program: Collaborative science on the ISS. In *IEEE Aerospace Conference Proceedings*, volume 1, pages 35–46, 2004.
- [8] Shinji Mitani, Masayuki Goto, Ryo Konomura, Yasushi Shoji, Keiji Hagiwara, Shuhei Shigeto, and Nobutaka Tanishima. Int-Ball: Crew-Supportive Autonomous Mobile Camera Robot on ISS/JEM. In *IEEE Aerospace Conference Proceedings*, volume 2019-March. IEEE Computer Society, 3 2019.
- [9] Maria G Bualat, Trey Smith, Terrence W Fong, Ernest E Smith, and D W Wheeler. Astrobe: A new tool for ISS operations. In *15th International Conference on Space Operations*, 2018, 2018.
- [10] Maria Bualat, Jonathan Barlow, Terrence Fong, Christopher Provencher, Trey Smith, and Allison Zuniga. Astrobe: Developing a free-flying robot for the international space station. In *AIAA SPACE 2015 Conference and Exposition*, 2015.
- [11] Aaron Parness, Neil Abcouwer, Christine Fuller, Nicholas Wiltsie, Jeremy Nash, and Brett Kennedy. LEMUR 3: A limbed climbing robot for extreme terrain mobility in space. In *Proceedings - IEEE International Conference on Robotics and Automation*, pages 5467–5473. Institute of Electrical and Electronics Engineers Inc., 7 2017.
- [12] Pablo Abad-Manterola, Joel Burdick, Issa A.D. Nesnas, and Johanna Cecava. Wheel design and tension analysis for the tethered axel rover on extreme terrain. In *IEEE Aerospace Conference Proceedings*, 2009.
- [13] S S Rao, T S Pan, and V B Venkayya. Modeling, Control, and Design of Flexible Structures: A Survey. *Applied Mechanics Reviews*, 43(5):99–117, 5 1990.
- [14] Rush Robinett III, Clark Dohrmann, G. Richard Eisler, John Feddema, Gordon Parker, David Wilson, and Dennis Stokes. *Flexible Robot Dynamics and Control*. Kluwer Academic/Plenum Publishers, 2002.
- [15] J. M. Martins, Z. Mohamed, M. O. Tokhi, J. Sá da Costa, and M. A. Botto. Approaches for dynamic modelling of flexible manipulator systems. In *IEEE Proceedings: Control Theory and Applications*, volume 150, pages 401–411, 7 2003.
- [16] Matthew A. Estrada, Benjamin Hockman, Andrew Bylard, Elliot W. Hawkes, Mark R. Cutkosky, and Marco Pavone. Free-flyer acquisition of spinning objects with gecko-inspired adhesives. *Proceedings - IEEE International Conference on Robotics and Automation*, 2016-June:4907–4913, 2016.
- [17] J Lorenzetti, B Landry, S Singh, and M Pavone. Reduced Order Model Predictive Control For Setpoint Tracking. In *2019 18th European Control Conference (ECC)*, pages 299–306, 6 2019.
- [18] Dynamics of Damped Cantilever Beam - MATLAB & Simulink.
- [19] Arnaud DeraeMaeker. *Dynamics of structures*. 2020.
- [20] Yuval Tassa, Tom Erez, and Emanuel Todorov. *Synthesis and Stabilization of Complex Behaviors through Online Trajectory Optimization*.